Available online at www.sciencedirect.com

SciVerse ScienceDirect

Scripta Materialia 68 (2013) 451–454

Scripta MATERIALIA

www.elsevier.com/locate/scriptamat

Phase field model of deformation twinning in tantalum: Parameterization via molecular dynamics

Yijia Gu,[a] Long-Qing Chen,[a] Tae Wook Heo,[a] Luis Sandoval[b,*] and James Belak[b]

[a]*Department of Materials Science and Engineering, The Pennsylvania State University, University Park, PA 16802, USA*
[b]*Condensed Matter and Materials, Lawrence Livermore National Laboratory, Livermore, CA 94550, USA*

Received 17 September 2012; revised 13 November 2012; accepted 14 November 2012
Available online 29 November 2012

We present a phase field model to simulate the microstructure evolution during deformation twinning in tantalum. An order parameter, proportional to the shear strain, is employed to monitor the twinning process. The evolution of the order parameter is governed by a time-dependent Ginzburg–Landau equation, the parameters of which are determined by molecular dynamics with a model-generalized pseudopotential-theory potential. The twinning process is studied under a number of deformation conditions, and compared with the molecular dynamics counterpart.

Keywords: Deformation structure; Twinning; Phase-field model; Molecular dynamics

Twinning is an important deformation mechanism which, like slip, involves dislocation activity. It plays a prominent role in plasticity under extreme conditions of low temperature or rapid loading [1,2]. After nucleation at stress concentrators in the material, the twin lamellae start to thicken. A variety of modeling techniques have been used to study this growth process, as a complete description of the phenomenon spans many time and length scales, from molecular dynamics [3] to continuum micromechanical models [4].

In this work we present a phase field model (PFM) for deformation twinning in the body-centered cubic (bcc) metal tantalum, similar to the model developed by Heo et al. [5] for face-centered cubic aluminum. The phase field model is parameterized with values calculated using molecular dynamics (MD) with a model-generalized pseudopotential-theory potential (MGPT) potential [6], thus bridging atomic/molecular scale and mesoscale simulations. In this study we focus on a two-dimensional (2-D) model, although it can be easily extended to the general 3-D case by using the appropriate gradient energy coefficient, which is defined below.

Twinning in bcc metals takes place on $\{1\,1\,2\}$ planes along the $\langle 1\,1\,1\rangle$ direction. It also has directionality, which has been explained through the minimum shear hypothesis [7], from where there only are 12 possible twinning modes.

The PFM 2-D computational cell is shown in Figure 1, which describes the process of deformation twinning as seen on the plane of shear $(0\,1\,1)$ [2]. Under these specifications there are only two possible twinning modes, which we have called variant 1 $((\bar{2}\,1\,1)[\bar{1}\,\bar{1}\,\bar{1}])$ and variant 2 $((2\,1\,1)[1\,\bar{1}\,\bar{1}])$. The corresponding habit planes are related via a rotation of $\theta = 70.53°$. A new coordinate system (x', y', z') is defined along the $[\bar{1}\,0\,0], [0\,\bar{1}\,\bar{1}]$ and $[0\,\bar{1}\,1]$, respectively, which is also used in the MD simulations.

As has been previously established [5], 2-D simulations on the $(0\,1\,\bar{1})$ plane requires only two order parameters, η_1 and η_2; that is, two spatially dependent fields, $\eta_1(r)$ and $\eta_2(r)$, are sufficient to describe the twinning microstructures (12 for a general 3-D case). If defined in the specifically chosen local reference frame (the x-axis is defined along the twinning direction, the y-axis is defined along the direction normal to habit plane and the z-axis is determined by right-hand rule), the pure shear strain tensor is

$$\epsilon_{i,j}^{1,ref} = \begin{pmatrix} 0 & s/2 & 0 \\ s/2 & 0 & 0 \\ 0 & 0 & 0 \end{pmatrix} \tag{1}$$

and

* Corresponding author. E-mail: sandoval28@llnl.gov

1359-6462/$ - see front matter © 2012 Acta Materialia Inc. Published by Elsevier Ltd. All rights reserved.
http://dx.doi.org/10.1016/j.scriptamat.2012.11.022

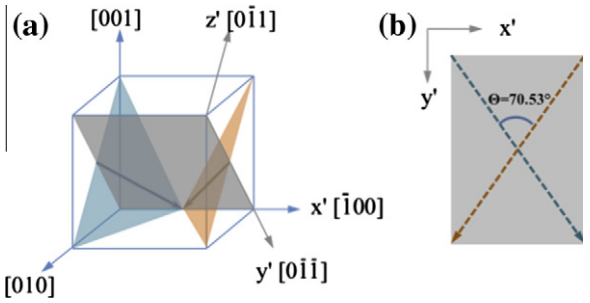

Figure 1. Crystallographic description of twinning for both variants (blue for variant 1, orange for variant 2). (a) Coordinate system set-up in a unit cell. (b) Configuration of the habit planes for both variants on the (0 1 1) plane. (For interpretation of the references to color in this figure legend, the reader is referred to the web version of this article.)

$$\epsilon_{i,j}^{2,ref} = \begin{pmatrix} 0 & -s/2 & 0 \\ -s/2 & 0 & 0 \\ 0 & 0 & 0 \end{pmatrix} \tag{2}$$

for variants 1 and 2, respectively, where $s = \sqrt{2}/2$ is the maximum magnitude of shear [2]. Transforming to the new coordinate system $(x'[\bar{1}\,0\,0], y'[0\,\bar{1}\,\bar{1}], z'[0\,\bar{1}\,1])$, we get, for both variants,

$$\epsilon_{i,j}^{1} = \begin{pmatrix} -\frac{s}{3} & \frac{s}{6\sqrt{2}} & 0 \\ \frac{s}{6\sqrt{2}} & \frac{s}{3} & 0 \\ 0 & 0 & 0 \end{pmatrix} \tag{3}$$

and

$$\epsilon_{i,j}^{2} = \begin{pmatrix} \frac{s}{3} & -\frac{s}{6\sqrt{2}} & 0 \\ -\frac{s}{6\sqrt{2}} & -\frac{s}{3} & 0 \\ 0 & 0 & 0 \end{pmatrix} \tag{4}$$

Assuming a linear dependence, the deformation strain tensor of variant p is then given by $\epsilon_{ij}^{(p)} = \eta_p \epsilon_{ij}^{p}$, where η_p is the order parameter describing the twinning process of variant p.

The evolution of order parameters is governed by the time-dependent Ginzburg–Landau (TDGL) equation,

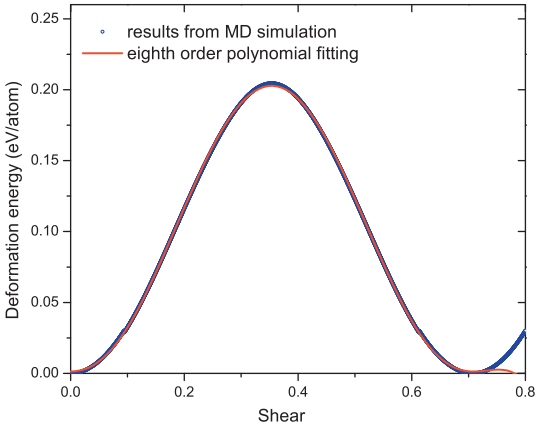

Figure 2. Deformation energy as a function of shear strain. The dashed line corresponds to an eighth-order polynomial fitting.

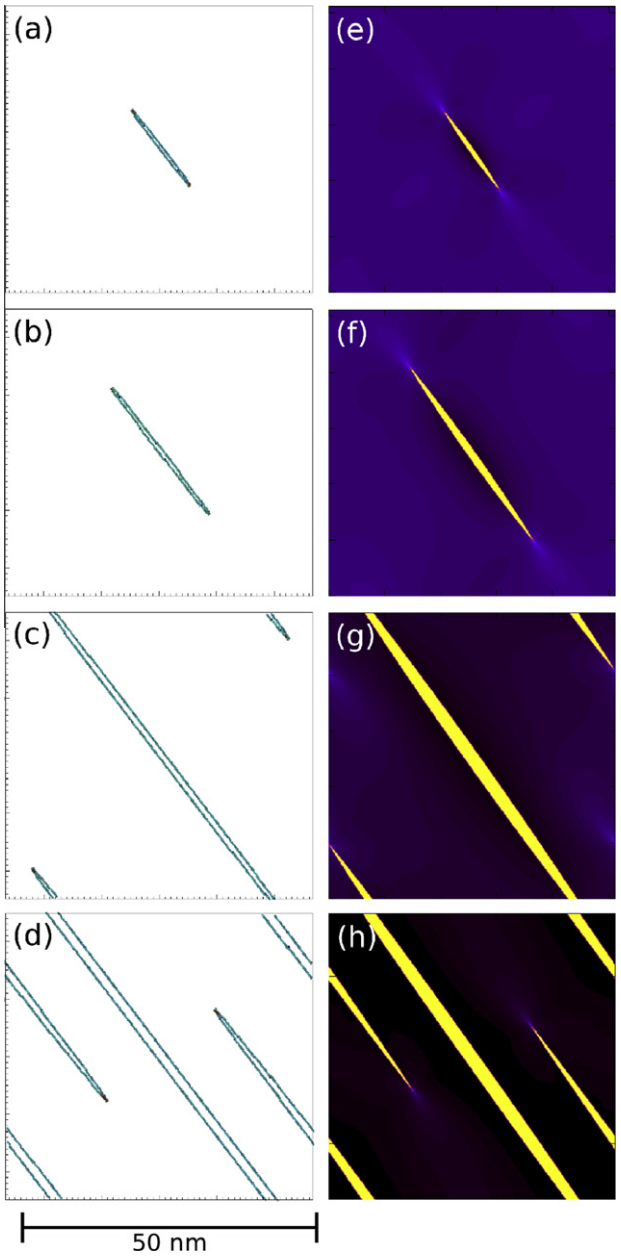

Figure 3. (a–d), MD simulations: (a) 2 ps, (b) 6 ps, (c) 18 ps, (d) 48 ps; (e–h), phase field simulations: (e) 1000 steps, (f) 5000 steps, (g) 15,000 steps, (h) 40,000 steps.

$$\begin{aligned} \frac{\partial \eta_p}{\partial t} &= -L\left(\frac{\delta F}{\delta \eta_p}\right) \\ &= -L\left(\frac{\partial f(\eta_p)}{\partial \eta_p} - \kappa_{p,ij}\nabla_i\nabla_j\eta_p + \frac{\partial E_{el}}{\partial \eta_p}\right) \end{aligned} \tag{5}$$

where t is time, F is the total free energy and L is the kinetic coefficient.

With the diffuse-interface description, the following volume integral gives the total free energy F of the system

$$F = \int_{\Omega}\left[f(\eta_1,\eta_2) + \sum_p \frac{\kappa_{ij}^{p}}{2}\nabla_i\eta_p\nabla_j\eta_p + \frac{1}{2}C_{ijkl}\left(\epsilon_{ij} - \epsilon_{ij}^{0}\right)\left(\epsilon_{kl} - \epsilon_{kl}^{0}\right)\right]\mathrm{d}V \tag{6}$$

where f is the local deformation energy density, κ_{ij}^{p} is the gradient energy coefficient tensor for the pth order parameter, C_{ijkl} is the elastic moduli, ϵ_{ij} is the local strain tensor, ϵ_{ij}^{0} is the eigenstrain tensor and Ω stands for the domain of interest. In order to bridge the phase field model and the MD, we get the energy function f, and the coefficients L, κ_{ij}^{p}, and C_{ijkl}, via MD simulations. The interatomic potential adopted in the MD simulations is a quantum-based, multi-body MGPT potential [6], which has been successfully applied to a broad range of temperatures, pressures and strains [8].

We computed the deformation energy along the twinning path via a homogeneous shear of the crystal, which is shown in Figure 2. At 0 GPa the energy barrier obtained has a value of 0.20 eV atom^{-1}, located at a shear strain value of $\sqrt{2}/4$, quite close to the first principles result of 0.197 eV atom^{-1} [9]. The curve was fitted, after normalization $f^{*} = \frac{f}{|\Delta f_{\max}|}$, to the eighth-order polynomial $f^{*} = A_0 + A_2(\eta - 0.5)^2 + A_4(\eta - 0.5)^4 + A_6 \quad (\eta - 0.5)^6 + \quad A_8(\eta - 0.5)^8$. The values of the coefficients are $A_0 = 1.0$, $A_2 = -11.1$, $A_4 = 46.9$, $A_6 = -96.2$ and $A_8 = 91.3$. For multiple variants we use $f^{*}(\eta_1, \eta_2) = f^{*}(\eta_1) + f^{*}(\eta_2) + A_c\eta_1^2\eta_2^2$, with $A_c = 80.0$ (value chosen to prevent overlapping of twinning variants).

The elastic moduli corresponding to the MGPT potential were calculated using a technique published recently [10], which allows us to find the three values with just a single simulation. The elastic moduli at 0 GPa are $C_{11} = 287.3$ GPa, $C_{12} = 189.8$ GPa and $C_{44} = 78.9$ GPa, which are relatively close to the experimental values of $C_{11}^{\exp} = 266.3$ GPa, $C_{12}^{\exp} = 158.2$ GPa and $C_{44}^{\exp} = 87.4$ GPa [11].

In a twinned structure the interface energy along the coherent twin boundaries is much smaller than the interfaces in other directions. In a 2-D system, this anisotropy is described by the gradient energy coefficient, which is defined as:

$$\kappa_{i,j}^{ref} = \begin{pmatrix} \kappa_{11} & 0 \\ 0 & \kappa_{22} \end{pmatrix} \tag{7}$$

where κ_{11} (incoherent twin boundaries) is larger than κ_{22} (coherent twin boundaries). The value of the interfacial energy corresponding to κ_{22}, determined via molecular dynamics using the MGPT potential, is 0.165 J m^{-2}, which, compared with the first-principles value of 0.217 J m^{-2}, provides an acceptable value. The calculation of the interfacial energy for the incoherent twin boundary is not trivial. As an approximation we take half of the surface energy [12], 1.6 J m^{-2}. By using $\gamma = \sqrt{2\kappa\Delta f}/3$, where γ is the interfacial energy [13], the gradient energy coefficient are calculated as $\kappa_{11} = 9.17 \times 10^{-10}$ J m^{-2}, and $\kappa_{22} = 9.71 \times 10^{-12}$ J m^{-2}.

The kinetic coefficient is the parameter which connects the real time scale to the simulation scale. An easy way to determine it is by assigning an initial value of 1, and running the phase field and MD simulation with the same twin nucleus and strain field. The MD simulations were performed in a box with dimensions 57 nm × 46 nm × 20 nm. The initial nucleus has the dimensions of 0.8 nm × 11.5 nm × 20 nm. A match between the phase field and MD simulations gives us a kinetic coefficient of $L = 461$ m^2 N^{-1} s^{-1}.

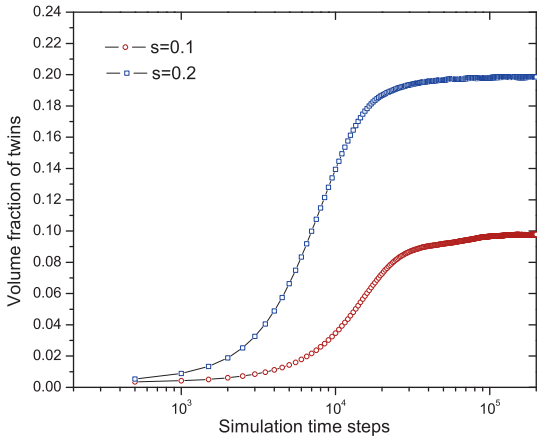

Figure 4. Volume fraction of twins as a function of simulation time.

The phase field simulations were performed in a square domain with $512\Delta x \times 512\Delta x$ grids, where Δx denotes the grid size, chosen to be 0.1 nm, with periodic boundary conditions. The parameters were normalized with the following expressions: $\Delta x^{*} = \Delta x/l$, $t^{*} = L|\Delta f_{\max}|t$, $\kappa_{ij}^{*} = \frac{\kappa_{ij}}{l^2|\Delta f_{\max}|}$, $C_{ij}^{*} = \frac{C_{ij}}{|\Delta f_{\max}|}$ and $f^{*} = \frac{f}{|\Delta f_{\max}|}$, where l is the characteristic length chosen to be equal to Δx. $|\Delta f_{\max}|$ is the maximum driving force obtained from the deformation energy curve. The values of the dimensionless normalized parameters are: $\Delta x^{*} = 1.0$, $t^{*} = 0.001$, $\kappa_{11}^{*} = 50.74$, $\kappa_{22}^{*} = 0.54$, $C_{11}^{*} = 159.0$, $C_{12}^{*} = 105.1$ and $C_{44}^{*} = 43.7$.

The volume average of the total eigenstrain should be equal to the homogeneous strain $\bar{\epsilon}_{ij}$. Therefore, we added a penalty term, $\frac{1}{2}\sum_{i,j} M_{ij}\left(\frac{1}{V}\int_{\Omega}\epsilon_{ij}^{0}\mathrm{d}V - \bar{\epsilon}_{ij}\right)^2$, to the free energy term, with $M_{11} = M_{22} = 1030$, $M_{12} = M_{21} = 3930$. The initial nucleus had an ellipsoidal shape, with a width of $8\Delta x$ and an aspect ratio of ~15, chosen to match the MD simulations.

In Figure 3 we show some snapshots corresponding to $0.1\epsilon_{ij}^{1}$. The PFM and MD simulations show a remarkable similarity, with a strong anisotropic behavior, given that the incoherent twin boundary growth is significantly faster than its coherent counterpart. It verifies the consistency of the governing equations for two different simulation approaches, i.e. the Liouville equation for MD and the TDGL equation for PFM.

In Figure 4 we show the volume fraction as a function of time. Since the slip deformation is not considered, the equilibrium volume fraction of twins is expected to be related to the macroscopic deformation, i.e. the homogeneous strain. In the growing process, as the driving force is the dissipation of deformation energy, the larger macroscopic deformation, the higher growth rate, as shown in the initial growth stage of the two cases.

A phase field model for deformation twinning in bcc metals, using tantalum as the representative material, has been built in order to simulate the microstructure evolution during deformation twinning. The evolution of the order parameter, proportional to the shear strain,

is governed by a time-dependent Ginzburg–Landau equation, the parameters of which were determined by MD with an MGPT potential. The twinning process is studied under a number of deformation conditions, and compared with the MD counterpart. The PFM and MD simulations show remarkable similarity, a sign of the excellent parameterization of the PFM, which can correctly reproduce the structural evolution of deformation twinning in terms of morphology and energy distribution.

The authors gratefully acknowledge Ming Tang, Robert Rudd, Michael Surh and David Richards for fruitful discussions. This work was performed under the auspices of the US Department of Energy by the Lawrence Livermore National Laboratory under contract DE-AC52-07NA27344 (LLNL-JRNL-581392) and the National Science Foundation under grant number DMR-0710483. The phase-field simulations were carried out on the LION and Cyberstar clusters at Pennsylvania State University, supported in part by NSF Major Research Instrumentation Program through grant number OCI-0821527, and in part by the Materials Simulation Center and the Graduated Education and Research Service at Pennsylvania State University.

[1] S.V. Lubenets, V.I. Startsev, L.S. Fomenko, Phys. Status Solidi A 92 (1985) 11.
[2] J.W. Christian, S. Mahajan, Prog. Mater. Sci. 39 (1995) 1.
[3] S. Ogata, J. Li, S. Yip, Phys. Rev. B 71 (2005) 224102.
[4] D.M. Kochmann, K.C. Le, J. Mech. Phys. Solids 57 (2009) 987.
[5] T.W. Heo, Y. Wang, S. Bhattacharya, X. Sun, S. Hu, L.-Q. Chen, Philos. Mag. Lett. 91 (2011) 110.
[6] J.A. Moriarty, J. Belak, R.E. Rudd, P. Soderlind, F.H. Streitz, L.H. Yang, J. Phys. Condens. Matter 14 (2002) 2825.
[7] M.A. Jaswon, D.B. Dove, Acta Crystallogr. 9 (1956) 621.
[8] C.J. Wu, P. Söderlind, J.N. Glosli, J.E. Klepeis, Nat. Mater. 8 (2009) 223.
[9] Y. Mishin, A. Lozovoi, Acta Mater. 54 (2006) 5013.
[10] M. Wen, A. Barnoush, K. Yokogawa, Comput. Phys. Commun. 182 (2011) 1621.
[11] G. Simmons, H. Wang, Single Crystal Elastic Constants and Calculated Aggregate Properties, MIT Press, Cambridge, MA, 1971.
[12] D.A. Porter, K.E. Easterling, M. Sherif, Phase Transformations in Metals and Alloys, third ed., CRC Press, Boca Raton, FL, 2009.
[13] L.-Q. Chen, Annu. Rev. Mater. Res. 32 (2002) 113.